Heparan sulfate regulates the number and centrosome positioning of *Drosophila* male germline stem cells

Daniel C. Levings, Takeshi Arashiro, and Hiroshi Nakato*
Department of Genetics, Cell Biology and Development, University of Minnesota, Minneapolis, MN 55455

ABSTRACT Stem cell division is tightly controlled via secreted signaling factors and cell adhesion molecules provided from local niche structures. Molecular mechanisms by which each niche component regulates stem cell behaviors remain to be elucidated. Here we show that heparan sulfate (HS), a class of glycosaminoglycan chains, regulates the number and asymmetric division of germline stem cells (GSCs) in the *Drosophila* testis. We found that GSC number is sensitive to the levels of 6-*O* sulfate groups on HS. Loss of 6-*O* sulfation also disrupted normal positioning of centrosomes, a process required for asymmetric division of GSCs. Blocking HS sulfation specifically in the niche, termed the hub, led to increased GSC numbers and mispositioning of centrosomes. The same treatment also perturbed the enrichment of Apc2, a component of the centrosome-anchoring machinery, at the hub–GSC interface. This perturbation of the centrosome-anchoring process ultimately led to an increase in the rate of spindle misorientation and symmetric GSC division. This study shows that specific HS modifications provide a novel regulatory mechanism for stem cell asymmetric division. The results also suggest that HS-mediated niche signaling acts upstream of GSC division orientation control.

Monitoring Editor
Yukiko Yamashita
University of Michigan

Received: Jul 27, 2015
Revised: Jan 11, 2016
Accepted: Jan 12, 2016

INTRODUCTION

Adult stem cells have the unique potential to divide and produce both stem and differentiating daughter cells over the life of an organism (He *et al.*, 2009). The differentiating cells produced in these divisions can go on to replace old or damaged tissue cells in response to aging, organ damage, or normal tissue homeostasis (Potten and Loeffler, 1990). A balance of production between stem and differentiating cells is of the utmost importance in ensuring that enough cells are present to carry out these processes while preventing excess cell output or cancer (Preston-Martin *et al.*, 1990). To maintain this balance, stem cells are regulated through both cell-intrinsic and -extrinsic mechanisms (He *et al.*, 2009). One such mechanism is asymmetric division, in which daughter cells are produced in a precisely oriented manner to maintain one stem cell in the niche while the other daughter cell moves away from it (Yamashita *et al.*, 2010; Inaba and Yamashita, 2012).

The germline stem cell (GSC) niche in the *Drosophila* testis offers an excellent system for studying stem cell maintenance and asymmetric division (Yamashita and Fuller, 2008; Yuan and Yamashita, 2010). In this niche, two populations of stem cells exist: GSCs and cyst stem cells (CySCs), which are a pair of somatic cells that enwrap each GSC. Both of these stem cell populations contact the niche, a group of somatic cells called the hub. Two key processes in the GSC niche regulate self-renewal and differentiation. First, the hub secretes the ligands Unpaired (Upd) and Glass bottom boat/Decapentaplegic (bone morphogenetic proteins [BMPs]), which are necessary for the maintenance of CySCs and GSCs, respectively (de Cuevas and Matunis, 2011). Second, E-cadherin (E-cad)–mediated adhesion allows for anchoring of centrosomes at the niche interface in GSCs (Yamashita *et al.*, 2003). This centrosome anchoring defines the future orientation of the spindle, which is perpendicular to the contact interface between each GSC and the hub, ensuring their stereotypical asymmetric division. Asymmetric division (mediated by centrosome anchoring) is a robust process in this niche, as GSC numbers must be tightly regulated to ensure renewal of the stem cell while also producing a single differentiating daughter cell,

This article was published online ahead of print in MBoC in Press (http://www.molbiolcell.org/cgi/doi/10.1091/mbc.E15-07-0528) on January 20, 2016.

*Address correspondence to: Hiroshi Nakato (nakat003@umn.edu).

Abbreviations used: Apc2, Adenomatous polyposis coli 2; COC, centrosome orientation checkpoint; CySC, cyst stem cell; GSC, germline stem cell; HS, heparan sulfate; HSPG, heparan sulfate proteoglycan; Hts, Hu-li tai shao; Sfl, Sulfateless; Ttv, Tout-velu; Upd, Unpaired.

called a gonialblast. In fact, proper anchoring of the mother centrosome in GSCs is typically essential for division to proceed (Yamashita *et al.*, 2005, 2007). The microtubule-binding protein Adenomatous polyposis coli 2 (Apc2) is important in this process. Apc2 preferentially localizes to the GSC cortex adjacent to the hub and participates in anchoring at this interface through its interactions with the mother centrosome's astral microtubules (Yamashita *et al.*, 2003). Of note, disruption or loss of Apc2 results in a premitotic arrest of GSC division. However, the relationship between these two mechanisms—niche signaling and division orientation control—is poorly understood.

One class of molecules that might play key roles in the stem cell niche are the carbohydrate-modified proteins heparan sulfate proteoglycans (HSPGs). HSPGs bind a number of ligand proteins via heparan sulfate (HS) chains to regulate their distribution and signaling (Bishop *et al.*, 2007). Such HS-dependent factors include fibroblast growth factors (FGFs), Wnts, BMPs, Hedgehog (Hh), and a *Drosophila* JAK/STAT ligand, Upd. Of importance, the fine structure of HS chains has a major effect on HSPG function (Nakato and Kimata, 2002; Kamimura *et al.*, 2011). During its biosynthesis, HS undergoes sequential modification events, including 6-*O* sulfation catalyzed by HS 6-*O* sulfotransferases (Hs6sts). After the HS modification steps occur in the Golgi, HS can be further modified extracellularly by a family of extracellular HS 6-*O* endosulfatases (Sulfs), which remove 6-*O* sulfate groups (Dhoot *et al.*, 2001). Functional studies of vertebrate and *Drosophila* Hs6sts and Sulfs show that they regulate Wnt, FGF, BMP, and Hh signaling (Kamimura *et al.*, 2001, 2006; Ai *et al.*, 2003; Habuchi and Kimata, 2010; Kleinschmit *et al.*, 2010, 2013; Wojcinski *et al.*, 2011), highlighting 6-*O* sulfation/desulfation as key regulatory steps for HS function.

We demonstrated that HSPGs are essential regulators of the GSC niche in the *Drosophila* ovary (Hayashi *et al.*, 2009). In the female GSC niche, HSPGs expressed in the niche (cap cells) activate BMP signaling in-*trans* in the directly contacting GSCs. This *trans* coreceptor activity of HSPGs can explain the contact dependence of GSC maintenance (Hayashi *et al.*, 2009; Dejima *et al.*, 2011). We also observed that GSCs and germ cells are substantially reduced in larval testes mutant for an essential HS biosynthetic gene, *tout-velu* (*ttv*; Hayashi *et al.*, 2009). Although this finding indicated essential roles of HS in the male GSC niche, the mechanism by which HS controls GSC maintenance is unknown. In this study, we addressed three major questions regarding the role of HS in regulation of male GSCs: 1) whether specific HS modifications play roles in the GSC niche, 2) in which cells does HS function, and 3) whether HS participates in asymmetric division in addition to niche signaling. Our findings suggest that HSPG-dependent signaling from the niche affects formation or function of the centrosome-anchoring complex at the hub–GSC interface and thus affects the division orientation of GSCs.

RESULTS AND DISCUSSION

Specific modifications of HS affect GSC numbers

To elucidate the mechanism by which HS regulates the male GSC niche, we asked whether HS modifications affect GSC numbers. We particularly focused on the role of the 6-*O* sulfate group, a key component of the binding sites on HS for most protein ligands (Ai *et al.*, 2003; Wojcinski *et al.*, 2011; Kleinschmit *et al.*, 2013).

Consistent with previous studies, wild-type testes had an average of 9–10 GSCs at 1–3 d posteclosion (Figure 1, A and D; Yamashita *et al.*, 2005; de Cuevas and Matunis, 2011). Of interest, homozygous *Hs6st*-null mutants had a significantly higher number of GSCs (Figure 1, B and D), but normal hub size and structure (Figure 1E), compared with both wild-type and heterozygous control flies. Anti–Hu-li tai shao (Hts) staining of the excess germ cells in *Hs6st* testes showed the spherical spectrosomes characteristic of a GSC/gonialblast (Figure 1F), confirming the undifferentiated status of these cells. Conversely, null mutants for *Sulf1* (the enzyme removing 6-*O* sulfation) had GSC numbers lower than that of the wild-type strain (Figure 1, C and D). These results indicate that HS 6-*O* sulfation levels affect GSC numbers.

Proper HS modification is required for normal GSC centrosome positioning

One possible explanation for the observed increase in GSC number is the failure of GSC asymmetric division. If a GSC division produces two daughter cells contacting the hub, both would be maintained as GSCs. In fact, abnormalities in stem cell number frequently accompany asymmetric division defects (Yamashita *et al.*, 2003; Lu *et al.*, 2012). Proper centrosome positioning is critical in this process. Specifically, the apical or mother centrosome in GSCs associates with components of the centrosome-anchoring machinery, such as Baz and Apc2 (Yamashita *et al.*, 2003; Inaba *et al.*, 2015), which are found at regions of the cell cortex with E-cad–mediated adhesion to the hub. The daughter centrosome migrates to the opposite side of the cell for division, and thus an axis perpendicular to the hub interface is established for spindle assembly.

We asked whether 6-*O* sulfation affects centrosome positioning in GSCs. Because the mother centrosome is normally anchored at the niche interface, any GSC with at least one centrosome at the 90° interface with the hub was counted as "oriented," and any GSC with neither centrosome at this interface was counted as "misoriented" (Figure 2, A–E). In wild type, mispositioning of centrosomes was observed in 14.4% of GSCs (Figure 2F). We found that *Hs6st*-null mutation results in a significant increase in the rate of centrosome mispositioning (34.5%) in GSCs compared with wild-type testes (Figure 2F). Thus proper 6-*O* sulfation is required for normal rates of oriented centrosomes in GSCs. No significant abnormality in centrosome positioning was observed in *Sulf1* mutants.

HS in the hub plays an important role in GSC number control

We next examined the cell type–specific requirement of HS in control of GSC number. To block HS biosynthesis, we used RNA interference (RNAi) knockdown of Sulfateless (Sfl), which catalyzes the first step of HS modification. Loss of *sfl* eliminates HS activity, and *sfl*-null mutants are larval lethal (Lin and Perrimon, 1999). We therefore disrupted *sfl* in specific cell types in the testis only at adult stages using the TARGET system, which allows temporal and spatial control of gene expression (McGuire *et al.*, 2003).

When we induced expression of a *sfl* short hairpin RNAi construct (*UAS-sh-sfl*) in the hub using *upd-Gal4*, GSC number was significantly increased compared with the isogenic control strain (Figure 3A and Supplemental Figure S1, A and B). This effect was similar to the phenotype observed in *Hs6st* mutants (Figure 1D). However, no significant change in GSC number was caused by knockdown of *sfl* in the germ cell or the CySC/CyC populations (Figure 3A and Supplemental Figure S1, C–F). These results suggest that HS expressed in the hub non–cell autonomously regulates GSC number.

We confirmed this result using the technique of germline-specific knockout (Kirchner *et al.*, 2008; White-Cooper, 2012). In this experiment, we used another critical gene for HS biosynthesis, *tout-velu (ttv)*, which encodes a HS copolymerase (Bellaiche *et al.*, 1998). *ttv* mutants have no detectable HS and are larval lethal (Toyoda *et al.*, 2000). We rescued these mutants by expressing *UAS-ttv* in all

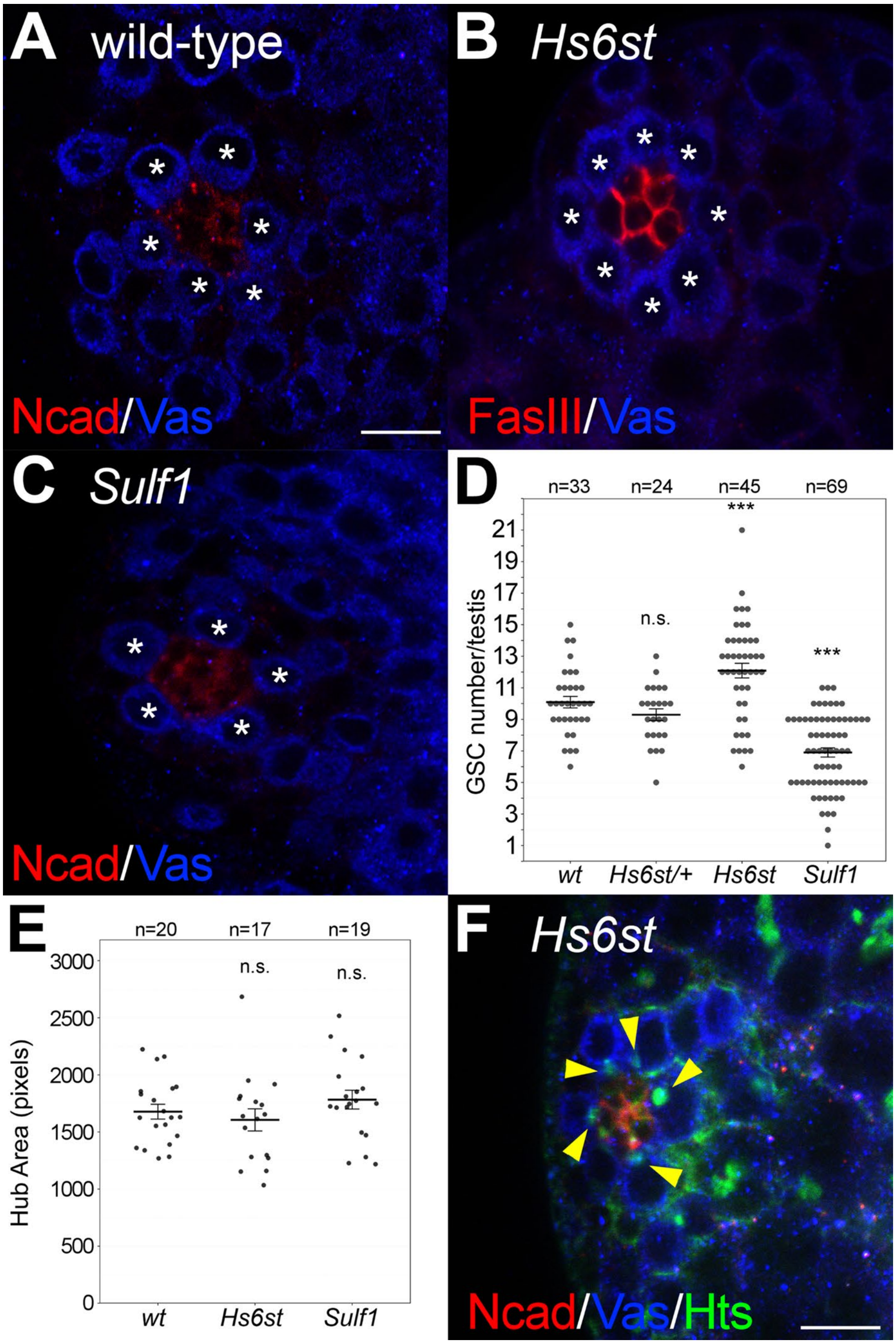

FIGURE 1: HS modifications regulate GSC number. (A–C) GSCs in a single confocal section in wild-type (A), *Hs6st* (B), and *Sulf1* (C) mutant testes. GSCs identified in these confocal sections are marked by asterisks. (D) Quantification of GSC numbers in *Hs6st* and *Sulf1* mutants. A cumulative count of all GSCs from multiple confocal sections was tallied for each testis. (E) Comparison of hub area. There is no significant difference in hub area in *Hs6st* and *Sulf1*. There is also no significant difference in hub diameter (length along the longest axis), perimeter length, or hub cell size between these genotypes (unpublished data). (F) Germ cells directly contacting the hub in *Hs6st* mutants have round spectrosomes (yellow arrowheads), which are characteristic of GSCs/gonialblasts. Numerical values are the mean ± SE. n.s., not significant; $^{***}p < 0.001$. *n*, number of testes assayed. Bar, 10 μm.

somatic cells but not germ cells, using *arm-Gal4*. The somatic cell–specific rescued animals (*ttv/ttv*; *arm>ttv*) survived to adult stages. These animals exhibited normal overall testis morphology and niche organization, with GSC numbers slightly lower than that of the reference wild-type strain (Figures 1A and 3C and Supplemental Figure S1G) but within the normal wild-type range, as well as normal centrosome positioning (Figures 2C and 3, B and D). On the basis of these results, we concluded that hub HS is responsible for regulation of GSC number.

Previous studies highlighted the importance of HS in maintenance of GSCs in both males and females (Hayashi *et al.*, 2009). For instance, in larvae with ubiquitous *ttv* loss (which do not survive to adulthood), GSCs are no longer maintained in the niche, and differentiating gonialblasts are observed contacting the niche. On the other hand, here we showed that loss or down-regulation of hub-specific HS or 6-*O* sulfation can result in increased GSC numbers in the male niche. One explanation is that HSPGs expressed in other cell populations, such as the CySCs, may partially rescue GSC maintenance but not hub-specific asymmetric division processes. As another possibility, reduction but not total elimination of hub HS may compromise some of its biological functions while still allowing sufficient signaling for GSC maintenance. Indeed, we did see GSC loss from the niche after long-term *sfl* knockdown (>12 d; unpublished data).

Hub-specific knockdown of HS perturbs normal centrosome positioning

To determine whether the increased number of GSCs caused by hub-specific HS loss is associated with abnormal orientation of GSC division, we examined centrosome positioning in *upd>sh-sfl* testes. We found that *sfl* knockdown in the hub led to a substantial increase in the rate of centrosome mispositioning (38.0%) compared with the RNAi control (17.3%; Figure 3E and Supplemental Figure S1, H and I).

Our analyses indicate that 1) hub HS is critical for normal centrosome anchoring and 2) 6-*O* sulfation is an essential modification step for this function of HS. To further confirm these results, we asked whether hub-specific loss of 6-*O* sulfation leads to a similar phenotype. We overexpressed a Golgi-tethered form of Sulf1 in the hub (*upd>Sulf1[Golgi]*), which removes 6-*O* sulfate groups in a cell-autonomous manner (Kleinschmit *et al.*, 2010). We found that the centrosome mispositioning rate in GSCs of *upd>Sulf1[Golgi]* (33.1%) recapitulated that of *upd>sh-sfl* (Figure 3E and Supplemental Figure S1J).

If HS expressed in the hub is responsible for anchoring centrosomes at the hub–GSC interface, then overexpression of HSPGs outside the niche could also disrupt centrosome positioning. To examine this idea, we expressed Dally (one of the glypican-class

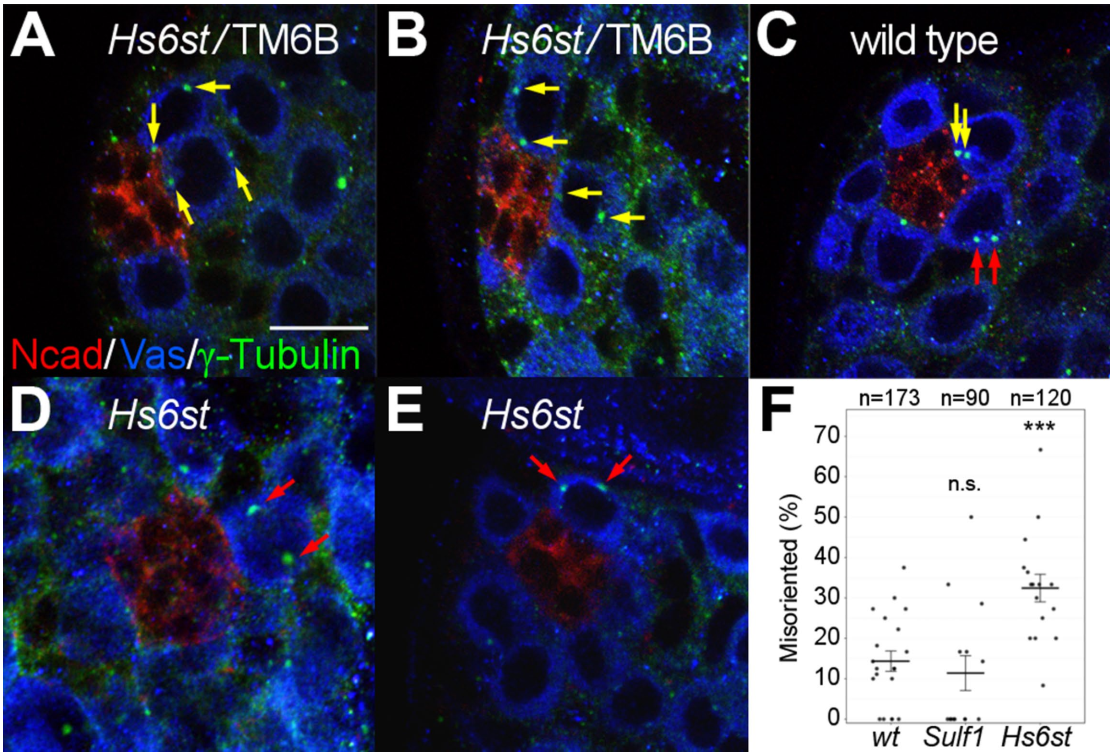

FIGURE 2: *Hs6st* mutation perturbs centrosome positioning in GSCs. (A–E) Centrosome positioning in GSCs. Examples are shown for pairs of properly oriented (yellow arrows) and misoriented (red arrows) centrosomes. Examples are shown from *Hs6st/TM6B* (A, B), wild-type (C), or *Hs6st* (D, E) testes. (F) Quantification of misoriented centrosomes (mean ± SE). n.s not significant; ****p* < 0.001. *n*, number of GSCs assayed. Bar, 10 μm.

HSPGs in *Drosophila*) in the CySC/CyC population. In this experiment, we also observed a significant increase in the rate of centrosome mispositioning (32.4%; Figure 3F and Supplemental Figure S1, K and L). This result supports the idea that HS on the surface of nearby, contacting cells provides GSCs with an orientation cue.

Loss of hub HS eliminates Apc2 enrichment at hub–GSC interface

To determine the mechanism for how hub HS regulates positioning of centrosomes in GSCs, we asked whether hub-specific loss of HS affects the centrosome-anchoring machinery. Previous studies identified Apc2 as a component of the cell membrane complex required for centrosome anchoring (Yamashita *et al.*, 2003; Venkei and Yamashita, 2015; Lu *et al.*, 2012). Apc2 anchors astral microtubules of the mother centrosome by directly or indirectly binding adherens junction components at the GSC interface with the hub, although the specific upstream partner(s) in this anchoring are not known (Inaba *et al.*, 2010). In the absence of Apc2, centrosomes are not properly anchored and a checkpoint arrests GSCs before spindle assembly.

We examined whether hub HS affects the localization of Apc2, a representative centrosome-anchoring component. In wild type, Apc2 was detected along the cell membrane with obvious enrichment at the hub–GSC interface (Figure 4, A and A′). Testes from the RNAi control showed a similar trend (Figure 4, C and C′). This pattern of Apc2 distribution was disrupted in *Hs6st* and *upd>sh-sfl* testes. The GSCs in these testes showed a more uniformly distributed Apc2 staining along the entire cell surface, with no obvious enrichment at the hub interface (Figure 4, B, B′, D, and D′). In addition, more diffusive cortical patterns of Apc2 staining were detected, leading to broader signals near the cell membrane, as observed in testes with germline-specific perturbation of insulin signaling (Roth *et al.*, 2012), Rac1 (Lu *et al.*, 2012), or Lar (Srinivasan *et al.*, 2012) activity.

To confirm these results, we quantified Apc2 distribution. We labeled GSCs with an anti-Apc2 antibody and measured the average staining intensity in the GSC cortex, specifically at the regions in contact with the hub and also the remaining GSC cortex (Figure 4E). In wild-type testes, GSCs showed a significant enrichment of Apc2 at the hub interface (Figure 4F). The quantification confirmed that both *sfl* knockdown in the hub and *Hs6st* mutation caused redistribution of Apc2. Specifically, hub enrichment of Apc2 was markedly reduced in both genotypes compared with controls (Figure 4, F and G). Taken together, these results strongly suggest that HS expressed in the hub is required for normal localization and function of the centrosome-anchoring machinery.

Loss of 6-*O* sulfation can disrupt spindle orientation and asymmetric division

Loss of proper centrosome anchoring, and thus positioning, generally activates the centrosome orientation checkpoint (COC; Cheng *et al.*, 2008; Inaba *et al.*, 2010). The COC halts division of wild-type GSCs in the G2 phase of the cell cycle, before spindle assembly and mitosis (Venkei and Yamashita, 2015). To date, only a few genetic manipulations have been able to bypass the COC and result in misoriented mitotic spindles, thus increasing the rate of symmetric division of GSCs. In many of these cases, genetic manipulations of components of the COC itself were used, such as Par-1 and Baz (Yuan *et al.*, 2012; Inaba *et al.*, 2015). The increased number of GSCs observed in *Hs6st* mutants suggests that *Hs6st* is a novel mutant that

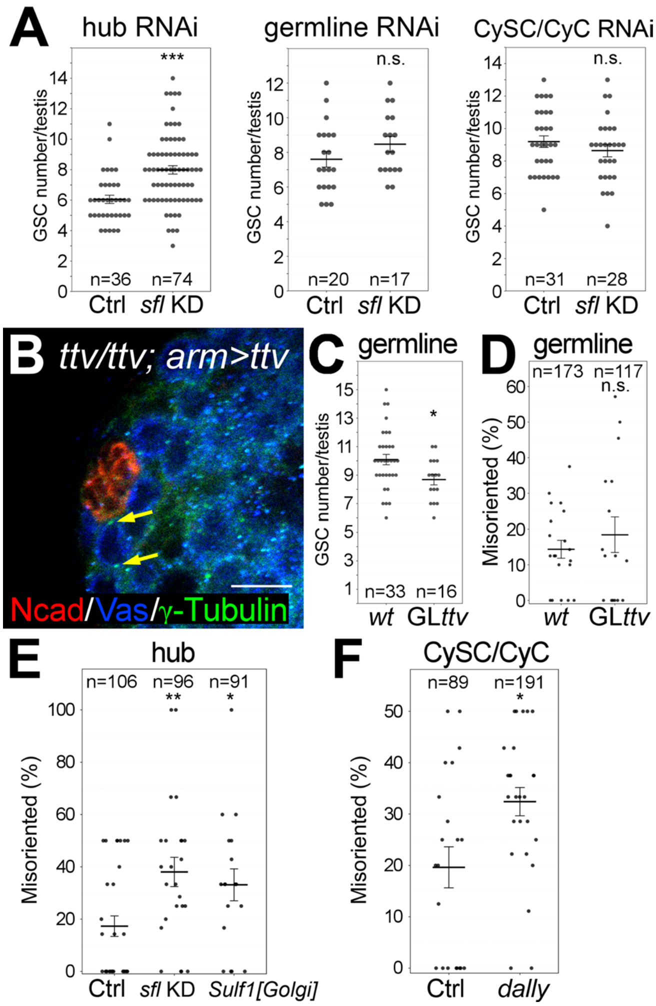

FIGURE 3: Hub HS is responsible for GSC number regulation and centrosome positioning. (A) GSC numbers for *sfl* TARGET knockdown animals. *UAS-sh-sfl* was driven by *upd-Gal4* (hub RNAi), *nos-Gal4* (germline RNAi), and *c587-Gal4* (CySC/CyC RNAi). (B–D) Somatic rescue of HS loss shows normal niche organization. The rescued animals (*ttv/ttv; arm>ttv*, indicated as GLttv in C and D) exhibited normal overall testis morphology, niche organization (B), GSC numbers (C), and centrosome positioning (yellow arrows in B, quantified in D). (E) Quantification of GSCs with mispositioned centrosomes in *upd-Gal4*, *upd>sh-sfl* and *upd>Sulf1[Golgi]* testes. (F) Quantification of GSCs with mispositioned centrosomes in *c587-Gal4* and *c587>dally-Myc*. Numerical values are the mean ± SE. n.s., not significant; *$p < 0.05$, **$p < 0.01$, ***$p < 0.001$. *n*, number of testes (A, C) or GSCs (D–F) assayed. Bar, 10 μm.

can bypass the COC and cause increased rates of symmetric division. To test this idea, we examined spindles in dividing GSCs in *Hs6st* mutants.

The asymmetric division process in wild-type animals was very robust (Figure 5A), and, similar to previous reports, we observed no instances of misoriented spindles in these flies after examining >600 GSCs and 20 divisions (Figure 5C). Remarkably, however, we observed a significant proportion of aberrant or misoriented divisions in *Hs6st*-mutant animals (21.1% of divisions, or 0.5% of total GSCs; Figure 5C). Several of these included mitotic GSCs with clearly misoriented spindles (Figure 5B). Of these, at least one appeared to feature an "unanchored" (not adjacent to hub) monopolar spindle (Supplemental Movie S1).

A model: HSPGs participate in centrosome anchoring

HSPGs facilitate formation or stabilization of growth factor signaling complexes (Fujise *et al.*, 2003; Akiyama *et al.*, 2008). In the female GSC niche, HSPGs expressed in the niche cells function as *trans* coreceptors for niche factors, such as BMPs, to regulate the maintenance of the stem cells contacting the niche (Hayashi *et al.*, 2009). Here we demonstrate that hub HS also affects centrosome anchoring and asymmetric division of GSCs in the testis. Our results show that hub HS affects Apc2 distribution, suggesting a link between niche signaling and the centrosome-anchoring machinery. Thus HSPGs may directly or indirectly participate in formation of a membrane complex at the niche–GSC interface, which recruits components of the centrosome-anchoring machinery to this region (Figure 5D).

The observed misorientation of spindles in animals with perturbed HS function, along with increased rates of centrosome mispositioning, indicates a failure in the asymmetric division of these stem cells. This increased rate of symmetric division likely explains the increased numbers of GSCs seen in *Hs6st* mutants and hub-specific knockdown of *sfl*. However, some questions remain, such as the mechanism by which these mutants bypass the COC and allow for GSC division despite a loss of proper centrosome anchoring.

One possibility is that HS controls localization of proteins necessary for centrosome anchoring/asymmetric cell division at specific regions of the GSC cortex, thus providing a "polarization signal." Other studies showed HSPGs to be capable of such a mechanism in a cell-autonomous manner (Dejima *et al.*, 2014). Here we propose that HS on the hub affects distribution of niche factor(s), such as Upd/BMP, and/or their receptor(s) by "tethering" these factors to the hub. Similar mechanisms have been shown in which HSPGs limit the diffusion of ligand proteins away from their source (Hayashi *et al.*, 2012). Because signaling events on the membrane of stem cells at the niche should inherently provide positional information about the extracellular environment of these cells, these signals may also trigger intracellular positional cues for the division machinery. Specifically, this tethering of niche factors to hub HS leads to the formation of the niche factor signaling complex *only* at the hub–GSC interface, causing a polarity in the GSC membrane. Thus, in wild type, the localized formation of the signaling complex allows for anchoring of the centrosome at this interface (Figure 5D). Under conditions of whole-animal loss of 6-*O* sulfation or loss of sulfation in the hub, this normal sequestration of niche factors at the hub may be lost and result in an expanded range of niche signaling. HS outside the niche, such as on the surface of CySCs/GSCs, appears to allow for ectopic signaling, which can lead to bypass of the COC in a fraction of misoriented GSCs (Figure 5E). Additional study is required to determine whether expanded niche signaling and ectopic localization of other centrosome-anchoring components are detected in these mutant and knockdown animals.

MATERIALS AND METHODS

Fly strains

Detailed information for the fly strains used is given at FlyBase (http://flybase.bio.indiana.edu/), except where noted. The wild-type strain used was Canton S. Other strains used were $Hs6st^{d770}$, a null allele of *Hs6st* (Kamimura *et al.*, 2006); $Sulf1^{dP1}$, a null allele of *Sulf1* (Kleinschmit *et al.*, 2010); ttv^{524}, a null allele of *ttv* (Takei *et al.*, 2004); *unpaired (upd)-Gal4* (Halder *et al.*, 1995); *nanos (nos)-Gal4 VP16* (Van Doren *et al.*, 1998); *c587-Gal4* (Kai and Spradling, 2003); *armadillo (arm)-Gal4* (Sanson *et al.*, 1996); *tubulin (tub)-*$Gal80^{ts}$ (McGuire *et al.*, 2003); *UAS-ttv* (The *et al.*, 1999); *UAS-dally-Myc* (Takeo *et al.*, 2005); *UAS-sh-sfl*, a UAS short hairpin RNAi strain for

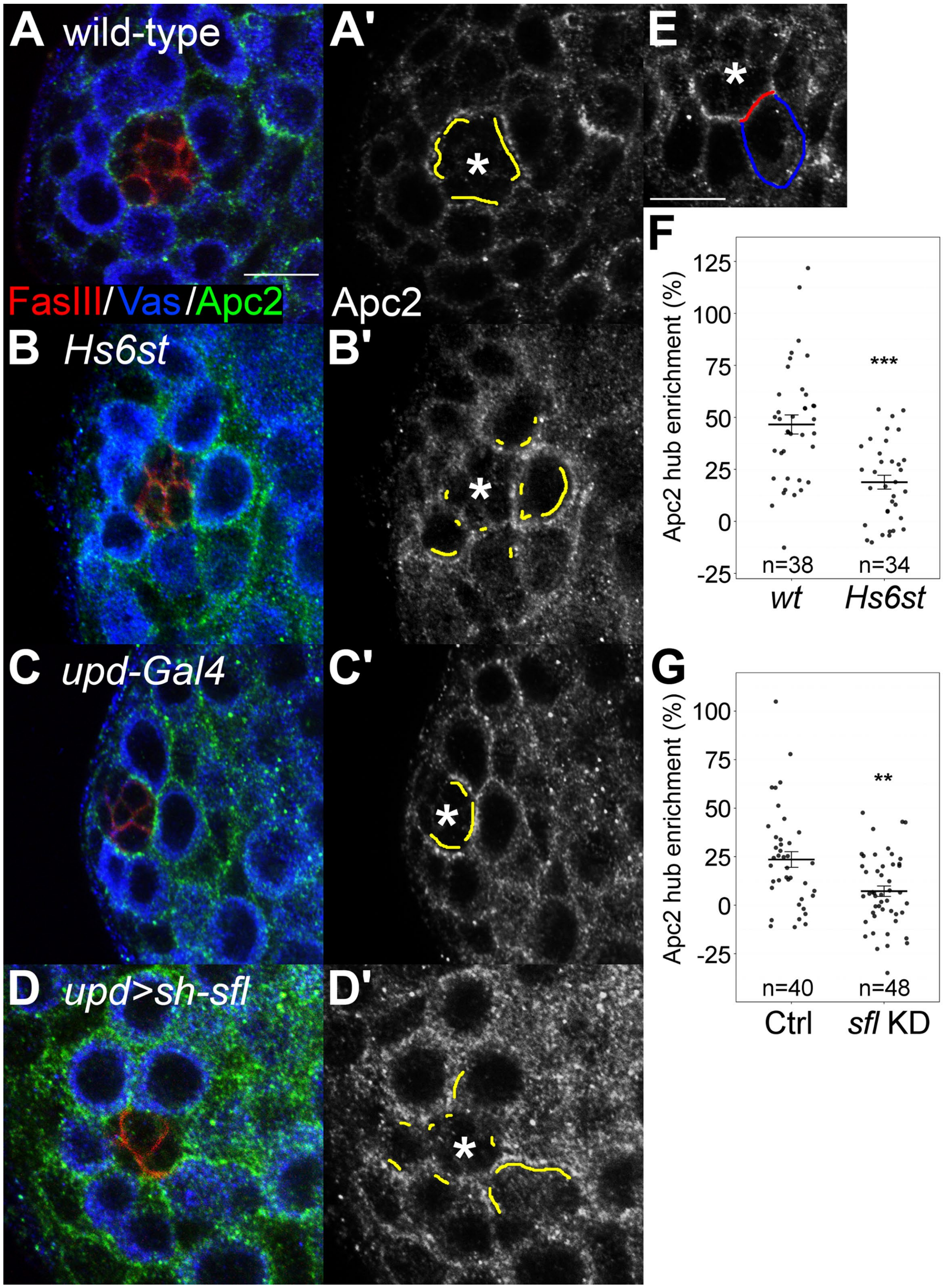

FIGURE 4: Hub HS regulates Apc2 distribution in GSCs. (A–D′) Apc2 localization (green in A–D and gray in A′–D′) in wild-type (A, A′), *Hs6st* mutants (B, B′), *upd-Gal4* (C, C′), and *upd>sh-sfl* (D, D′) testes. Hub (FasIII) and germline cells (Vas) are shown in red and blue, respectively (A–D). Positions of hubs are marked by asterisks, and strong Apc2 signals are highlighted by yellow lines (A′–D′). (E–G) Quantification of Apc2 enrichment. The hub–GSC interface and the remaining GSC cortex are shown by red and blue lines, respectively (E). *Hs6st* mutation (F) and hub-specific knockdown of *sfl* (G) disrupted Apc2 localization to the interface, resulting in a significant loss of Apc2 enrichment at the hub interface (F, G). Numerical values are the mean ± SE. *n*, number of GSCs assayed. **$p < 0.01$, ***$p < 0.001$. Bar, 10 μm.

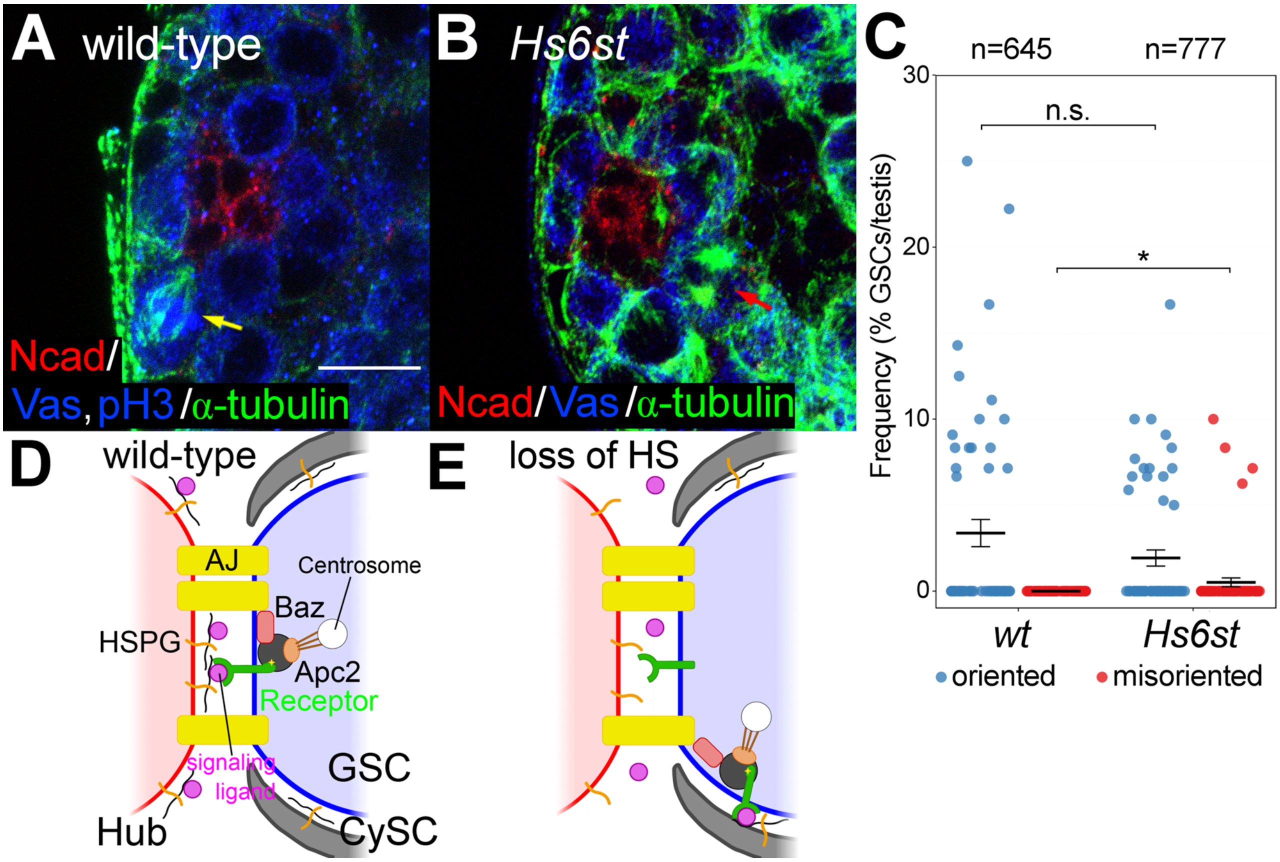

FIGURE 5: Misoriented spindle in dividing *Hs6st* GSCs. (A–C) Spindle orientation in GSCs. Examples are shown for properly oriented (yellow arrow) and misoriented (red arrow) spindles. No misoriented spindles were observed in wild type (A), whereas a significant fraction (21.1%) of dividing *Hs6st* GSCs showed misoriented (B) or aberrant spindles. $n = 20$ (wild type) and 19 (*Hs6st*) dividing GSCs counted. (C) Quantification of spindle orientation/misorientation. In wild type, the rates of spindle orientation vs. misorientation were 3.4 and 0% of GSCs, respectively. In *Hs6st* mutants, there was no significant difference in the rate of oriented divisions (1.9%) from wild type; however, a significantly higher rate of misoriented divisions was detected (0.5%). (D, E) Model for the role of HSPGs in centrosome anchoring. HSPGs may participate in formation of a membrane complex at the niche–GSC interface, which allows for a "polarization signal" and recruits components of the centrosome-anchoring machinery to this interface (D). When HS is lost, the signaling range of niche factor(s) involved in this process is expanded, resulting in mispositioning of centrosomes and misoriented division (E). Numerical values are the mean ± SE. *n*, number of GSCs assayed. n.s., not significant; $^*p < 0.05$. Bar, 10 μm.

sfl (Zhang *et al.*, 2013); and *P{CaryP}attP2*, an isogenic parent strain used for targeted insertion of TRiP short-hairpin constructs into the attP2 locus.

The TARGET (Gal4-Gal80^{ts}) system was used to induce *UAS-sh-sfl* expression in specific cell types of the adult testis (McGuire *et al.*, 2003; Kleinschmit *et al.*, 2013). For hub cell–specific knockdown, animals with the genotype of *upd-Gal4; tub-Gal80^{ts}/UAS-sh-sfl* were raised at the Gal80^{ts} permissive temperature (18°C). Adult flies were transferred to a new vial at 0–2 d after eclosion, the temperature was shifted to the Gal80^{ts} restrictive temperature (30°C), and the flies were incubated for an additional 6 d. Flies were transferred to fresh food at least once every 2 d. *nos-Gal4 VP16* and *c587-Gal4* (along with *tub-Gal80^{ts}*) were used for germline cell- and CySC/CyC-specific expression, respectively. The control strains used in each of these RNAi experiments were generated by crossing the respective Gal4 TARGET strain with the isogenic parent strain of the TRiP lines, *P{CaryP}attP2*. For example, hub RNAi control flies had the genotype *upd-Gal4; tub-Gal80^{ts}/P{CaryP}attP2*.

Germline-specific knockout

For the germline-specific knockout experiment, the fly stocks *ttv^{524}/CyO; arm-Gal4* and *ttv^{524}/CyO; UAS-ttv* were crossed at 25°C. The resulting *ttv^{524}; arm-Gal4/UAS-ttv* offspring had rescued *ttv* activity exclusively in the somatic cells of the animal but not the germline (Kirchner *et al.*, 2008; White-Cooper, 2012). Although loss of *ttv* is larval lethal, the rescued animals survived to adult stages. By allowing for normal fly development and HS function in the somatic hub and CySC/CyC lineages, we were able to investigate the role of HS loss specifically in the germline.

Immunofluorescence staining

Immunostaining was performed as previously described (Fujise *et al.*, 2001; Dejima *et al.*, 2013; Salzmann *et al.*, 2013). Briefly, samples were fixed for 30 min with 4% formaldehyde in phosphate-buffered saline (PBS), permeabilized in 0.3% PBST (0.3% Triton X-100 in PBS) for 20 min (10 min, twice), and washed with 0.1% PBST (10 min, twice). They were then blocked in 5% normal goat serum in 0.1% PBST for 1 h and incubated overnight in primary antibodies at 4°C. Samples were again washed in 0.1% PBST (10 min, three times) and incubated with the appropriate Alexa Fluor secondary antibodies either overnight at 4°C or for 2 h at room temperature. They were then washed in 0.1% PBST (10 min, four times) before being mounted in VECTASHIELD (H-1000 or H-1200; Vector Laboratories, Burlingame, CA).

For centrosome-positioning scoring experiments, samples were fixed for 1 h with 4% formaldehyde in PBS, permeabilized for 30 min in 0.3% sodium deoxycholate plus 0.3% PBST (15 min, twice), and washed with 0.1% PBST (10 min, twice). For Apc2 staining experiments, samples were prepared according to Srinivasan *et al.* (2012) with some modification. Briefly, samples were fixed for 20 min with 4% formaldehyde in PBS, permeabilized for 1 h in 0.6% sodium deoxycholate plus 0.3% PBST (20 min, three times), and washed with 0.1% PBST (10 min, twice). Images were obtained using either a Zeiss 710 or a Nikon Eclipse E800 laser scanning confocal microscope.

The following primary antibodies were used: rabbit anti-Vasa (Vas; 1:500; a gift from S. Kobayashi, Okazaki Institute for Integrative Bioscience, Okazaki, Japan), chick anti-Vas (1:1000; a gift from S. Kobayashi), mouse anti-Hts (1:5; Developmental Studies Hybridoma Bank [DSHB], University of Iowa, Iowa City, IA), rat anti–E-cad (1:40; DSHB), rat anti–N-cad (1:20; DSHB), mouse anti-FasIII (1:200; DSHB), mouse anti–γ-tubulin (GTU-88; 1:500; Sigma-Aldrich, St. Louis, MO), rabbit anti–phospho-histone H3 (Ser-10; 1:1000; EMD Millipore, Billerica, MA), and rabbit anti-Apc2 (1:5000; a gift from M. Bienz, MRC Laboratory of Molecular Biology, Cambridge, UK). Secondary antibodies were from the Alexa Fluor series (1:500; ThermoFisher Scientific, Waltham, MA).

Quantification of GSC number and hub measurement

GSCs were counted as described previously (Boyle *et al.*, 2007; Hayashi *et al.*, 2009; Srinivasan *et al.*, 2012). Germline cells were counted as stem cells only when directly contacting hub cells labeled with $FasIII^+$, $N\text{-}cad^+$, or $E\text{-}Cad^+$. In brief, a confocal microscope was used to scan through the samples, and a cumulative count of all Vas^+ germline cells contacting the hub was tallied for each testis. These numbers were then used to generate an average GSC number for each genotype (in each experiment). For most genotypes, GSC identity was also verified by spectrosome morphology (spherical Hts staining) in a subset of samples. This is a characteristic marker for GSCs and gonialblasts only, whereas a branched fusome morphology is seen by Hts staining in later stages of spermatogonial development. Briefly, while scanning through the depth of a sample, Hts staining was examined in each germline cell contacting the niche. If the Hts^+ organelle showed a small, spherical morphology, the germline cell was counted as a GSC (vs. a dumbbell-shaped or branched morphology characteristic of differentiating germline cells).

For measurement of hub area, images showing a cross section through the middle portion of each hub (with the largest cross-sectional diameter) were taken of each testis at the same magnification by confocal microscopy. ImageJ (National Institutes of Health, Bethesda, MD) was then used to trace around the circumference of the hub, as well as two or three individual hub cells, and the area of each hub/cell was calculated using the Measure function in ImageJ. The average hub and hub cell pixel area for each genotype were then calculated with Excel. A two-tailed Student's *t* test was used to determine statistical significance for both GSC number and hub/cell size.

Scoring of centrosome positioning, spindle orientation, and Apc2 distribution

GSC centrosome positioning was scored as "oriented" or "misoriented" as described previously (Cheng *et al.*, 2008). Briefly, any GSC for which either of the two centrosomes was observed at the 90° interface with the hub was counted as "oriented," and any GSC with neither centrosome found at this interface was counted as "misoriented." Of importance, if there was no centrosome anchoring, a single centrosome would be expected to randomly localize to this 90° interface ~25% of the time. Thus a centrosome-mispositioning rate of 50% is essentially random, since either centrosome could be found at this interface randomly ~25% of the time and result in a score of "oriented" (25% × 2 = 50%). Only GSCs with two clearly detectable centrosomes were counted. Spindles were also scored as "oriented" or "misoriented" according to the same criteria as centrosome orientation, except observing spindle poles instead of centrosomes, as described previously (Inaba *et al.*, 2015).

To quantify the Apc2 distribution patterns, we used a modified version of the line-tracing method for quantifying Apc2 intensity used by Roth *et al.* (2012). In brief, we first obtained images of many GSCs/niches of each genotype using confocal microscopy. In obtaining these images, the focal plane was adjusted to roughly bisect the hub while also bisecting several of the contacting GSCs. The signal intensity/gain for the Apc2 channel was adjusted to achieve maximal signal without saturation (since our goal was to compare distribution, not absolute protein levels). We then used ImageJ to trace the Apc2 signal intensity at the GSC interface with the hub ("interface"; red line, Figure 4D) separately from the rest of the GSC cortex ("periphery"; blue line, Figure 4D). To ensure unbiased measurement, we first defined positions of the interface versus the periphery using the Vas- and N-cad–stained channels from confocal images and traced a line along each of these membranes. After a switch to the Apc2 channel, the Apc2 intensity (averaged over a 5-pixel width) was measured separately along each of these lines for each GSC. The average Apc2 intensity for 1) the hub interface and 2) the hub interface added to the remaining (periphery) cortex was calculated for each GSC. The Apc2 hub enrichment was then calculated as the ratio of the average hub Apc2 intensity divided by the average cumulative Apc2 intensity minus one for each GSC. A two-tailed Student's *t* test was used for determining statistical significance for centrosome mispositioning, spindle orientation, and Apc2 hub enrichment.

ACKNOWLEDGMENTS

We are grateful to M. Bienz, S. Kobayashi, M. O'Connor, the Developmental Studies Hybridoma Bank, the Bloomington *Drosophila* Stock Center (Indiana University, Bloomington, IN), and the Transgenic RNAi Project at Harvard Medical School (Boston, MA) for fly stocks and reagents. We thank L. Hanson, K. Dejima, M. Takemura, and A. Toth for helpful discussions and critical reading of the manuscript. This work was supported by research grants from the National Institutes of Health (R01 GM115099).

REFERENCES

Ai X, Do AT, Lozynska O, Kusche-Gullberg M, Lindahl U, Emerson CP Jr (2003). QSulf1 remodels the 6-O sulfation states of cell surface heparan sulfate proteoglycans to promote Wnt signaling. J Cell Biol 162, 341–351.

Akiyama T, Kamimura K, Firkus C, Takeo S, Shimmi O, Nakato H (2008). Dally regulates Dpp morphogen gradient formation by stabilizing Dpp on the cell surface. Dev Biol 313, 408–419.

Bellaiche Y, The I, Perrimon N (1998). Tout-velu is a Drosophila homologue of the putative tumour suppressor EXT-1 and is needed for Hh diffusion. Nature 394, 85–88.

Bishop JR, Schuksz M, Esko JD (2007). Heparan sulphate proteoglycans fine-tune mammalian physiology. Nature 446, 1030–1037.

Boyle M, Wong C, Rocha M, Jones DL (2007). Decline in self-renewal factors contributes to aging of the stem cell niche in the Drosophila testis. Cell Stem Cell 1, 470–478.
Cheng J, Turkel N, Hemati N, Fuller MT, Hunt AJ, Yamashita YM (2008). Centrosome misorientation reduces stem cell division during ageing. Nature 456, 599–604.
de Cuevas M, Matunis EL (2011). The stem cell niche: lessons from the Drosophila testis. Development 138, 2861–2869.
Dejima K, Kanai MI, Akiyama T, Levings DC, Nakato H (2011). Novel contact-dependent bone morphogenetic protein (BMP) signaling mediated by heparan sulfate proteoglycans. J Biol Chem 286, 17103–17111.
Dejima K, Kang S, Mitani S, Cosman PC, Chisholm AD (2014). Syndecan defines precise spindle orientation by modulating Wnt signaling in C. elegans. Development 141, 4354–4365.
Dejima K, Kleinschmit A, Takemura M, Choi PY, Kinoshita-Toyoda A, Toyoda H, Nakato H (2013). The role of Drosophila heparan sulfate 6-o-endosulfatase in sulfation compensation. J Biol Chem 288, 6574–6582.
Dhoot GK, Gustafsson MK, Ai X, Sun W, Standiford DM, Emerson CP Jr (2001). Regulation of Wnt signaling and embryo patterning by an extracellular sulfatase. Science 293, 1663–1666.
Fujise M, Izumi S, Selleck SB, Nakato H (2001). Regulation of dally, an integral membrane proteoglycan, and its function during adult sensory organ formation of Drosophila. Dev Biol 235, 433–448.
Fujise M, Takeo S, Kamimura K, Matsuo T, Aigaki T, Izumi S, Nakato H (2003). Dally regulates Dpp morphogen gradient formation in the Drosophila wing. Development 130, 1515–1522.
Habuchi H, Kimata K (2010). Mice deficient in heparan sulfate 6-O-sulfotransferase-1. Prog Mol Biol Transl Sci 93, 79–111.
Halder G, Callaerts P, Gehring WJ (1995). Induction of ectopic eyes by targeted expression of the eyeless gene in Drosophila. Science 267, 1788–1792.
Hayashi Y, Kobayashi S, Nakato H (2009). Drosophila glypicans regulate the germline stem cell niche. J Cell Biol 187, 473–480.
Hayashi Y, Sexton TR, Dejima K, Perry DW, Takemura M, Kobayashi S, Nakato H, Harrison DA (2012). Glypicans regulate JAK/STAT signaling and distribution of the Unpaired morphogen. Development 139, 4162–4171.
He S, Nakada D, Morrison SJ (2009). Mechanisms of stem cell self-renewal. Annu Rev Cell Dev Biol 25, 377–406.
Inaba M, Venkei ZG, Yamashita YM (2015). The polarity protein Baz forms a platform for the centrosome orientation during asymmetric stem cell division in the Drosophila male germline. Elife 4, 04960.
Inaba M, Yamashita YM (2012). Asymmetric stem cell division: precision for robustness. Cell Stem Cell 11, 461–469.
Inaba M, Yuan H, Salzmann V, Fuller MT, Yamashita YM (2010). E-cadherin is required for centrosome and spindle orientation in Drosophila male germline stem cells. PLoS One 5, e12473.
Kai T, Spradling A (2003). An empty Drosophila stem cell niche reactivates the proliferation of ectopic cells. Proc Natl Acad Sci USA 100, 4633–4638.
Kamimura K, Fujise M, Villa F, Izumi S, Habuchi H, Kimata K, Nakato H (2001). Drosophila heparan sulfate 6-O-sulfotransferase (dHS6ST) gene. Structure, expression, and function in the formation of the tracheal system. J Biol Chem 276, 17014–17021.
Kamimura K, Koyama T, Habuchi H, Ueda R, Masu M, Kimata K, Nakato H (2006). Specific and flexible roles of heparan sulfate modifications in Drosophila FGF signaling. J Cell Biol 174, 773–778.
Kamimura K, Maeda N, Nakato H (2011). In vivo manipulation of heparan sulfate structure and its effect on Drosophila development. Glycobiology 21, 607–618.
Kirchner J, Vissi E, Gross S, Szoor B, Rudenko A, Alphey L, White-Cooper H (2008). Drosophila Uri, a PP1alpha binding protein, is essential for viability, maintenance of DNA integrity and normal transcriptional activity. BMC Mol Biol 9, 36.
Kleinschmit A, Koyama T, Dejima K, Hayashi Y, Kamimura K, Nakato H (2010). Drosophila heparan sulfate 6-O endosulfatase regulates Wingless morphogen gradient formation. Dev Biol 345, 204–214.
Kleinschmit A, Takemura M, Dejima K, Choi PY, Nakato H (2013). Drosophila heparan sulfate 6-O-endosulfatase Sulf1 facilitates wingless (Wg) protein degradation. J Biol Chem 288, 5081–5089.
Lin X, Perrimon N (1999). Dally cooperates with Drosophila Frizzled 2 to transduce Wingless signalling. Nature 400, 281–284.
Lu W, Casanueva MO, Mahowald AP, Kato M, Lauterbach D, Ferguson EL (2012). Niche-associated activation of rac promotes the asymmetric division of Drosophila female germline stem cells. PLoS Biol 10, e1001357.
McGuire SE, Le PT, Osborn AJ, Matsumoto K, Davis RL (2003). Spatiotemporal rescue of memory dysfunction in Drosophila. Science 302, 1765–1768.
Nakato H, Kimata K (2002). Heparan sulfate fine structure and specificity of proteoglycan functions. Biochim Biophys Acta 1573, 312–318.
Potten CS, Loeffler M (1990). Stem cells: attributes, cycles, spirals, pitfalls and uncertainties. Lessons for and from the crypt. Development 110, 1001–1020.
Preston-Martin S, Pike MC, Ross RK, Jones PA, Henderson BE (1990). Increased cell division as a cause of human cancer. Cancer Res 50, 7415–7421.
Roth TM, Chiang CY, Inaba M, Yuan H, Salzmann V, Roth CE, Yamashita YM (2012). Centrosome misorientation mediates slowing of the cell cycle under limited nutrient conditions in Drosophila male germline stem cells. Mol Biol Cell 23, 1524–1532.
Salzmann V, Inaba M, Cheng J, Yamashita YM (2013). Lineage tracing quantification reveals symmetric stem cell division in Drosophila male germline stem cells. Cell Mol Bioeng 6, 441–448.
Sanson B, White P, Vincent JP (1996). Uncoupling cadherin-based adhesion from wingless signalling in Drosophila. Nature 383, 627–630.
Srinivasan S, Mahowald AP, Fuller MT (2012). The receptor tyrosine phosphatase Lar regulates adhesion between Drosophila male germline stem cells and the niche. Development 139, 1381–1390.
Takei Y, Ozawa Y, Sato M, Watanabe A, Tabata T (2004). Three Drosophila EXT genes shape morphogen gradients through synthesis of heparan sulfate proteoglycans. Development 131, 73–82.
Takeo S, Akiyama T, Firkus C, Aigaki T, Nakato H (2005). Expression of a secreted form of Dally, a Drosophila glypican, induces overgrowth phenotype by affecting action range of Hedgehog. Dev Biol 284, 204–218.
The I, Bellaiche Y, Perrimon N (1999). Hedgehog movement is regulated through tout velu-dependent synthesis of a heparan sulfate proteoglycan. Mol Cell 4, 633–639.
Toyoda H, Kinoshita-Toyoda A, Fox B, Selleck SB (2000). Structural analysis of glycosaminoglycans in animals bearing mutations in sugarless, sulfateless, and tout-velu. Drosophila homologues of vertebrate genes encoding glycosaminoglycan biosynthetic enzymes. J Biol Chem 275, 21856–21861.
Van Doren M, Williamson AL, Lehmann R (1998). Regulation of zygotic gene expression in Drosophila primordial germ cells. Curr Biol 8, 243–246.
Venkei ZG, Yamashita YM (2015). The centrosome orientation checkpoint is germline stem cell specific and operates prior to the spindle assembly checkpoint in Drosophila testis. Development 142, 62–69.
White-Cooper H (2012). Tissue, cell type and stage-specific ectopic gene expression and RNAi induction in the Drosophila testis. Spermatogenesis 2, 11–22.
Wojcinski A, Nakato H, Soula C, Glise B (2011). DSulfatase-1 fine-tunes Hedgehog patterning activity through a novel regulatory feedback loop. Dev Biol 358, 168–180.
Yamashita YM, Fuller MT (2008). Asymmetric centrosome behavior and the mechanisms of stem cell division. J Cell Biol 180, 261–266.
Yamashita YM, Fuller MT, Jones DL (2005). Signaling in stem cell niches: lessons from the Drosophila germline. J Cell Sci 118, 665–672.
Yamashita YM, Jones DL, Fuller MT (2003). Orientation of asymmetric stem cell division by the APC tumor suppressor and centrosome. Science 301, 1547–1550.
Yamashita YM, Mahowald AP, Perlin JR, Fuller MT (2007). Asymmetric inheritance of mother versus daughter centrosome in stem cell division. Science 315, 518–521.
Yamashita YM, Yuan H, Cheng J, Hunt AJ (2010). Polarity in stem cell division: asymmetric stem cell division in tissue homeostasis. Cold Spring Harb Perspect Biol 2, a001313.
Yuan H, Chiang CY, Cheng J, Salzmann V, Yamashita YM (2012). Regulation of cyclin A localization downstream of Par-1 function is critical for the centrosome orientation checkpoint in Drosophila male germline stem cells. Dev Biol 361, 57–67.
Yuan H, Yamashita YM (2010). Germline stem cells: stems of the next generation. Curr Opin Cell Biol 22, 730–736.
Zhang Y, You J, Ren W, Lin X (2013). Drosophila glypicans Dally and Dally-like are essential regulators for JAK/STAT signaling and Unpaired distribution in eye development. Dev Biol 375, 23–32.